IEEE Access
Multidisciplinary | Rapid Review | Open Access Journal

Received May 24, 2019, accepted June 16, 2019, date of publication June 24, 2019, date of current version July 15, 2019.

Digital Object Identifier 10.1109/ACCESS.2019.2924464

A Robust Iris Segmentation Scheme Based on Improved U-Net

WEI ZHANG[1], XIAOQI LU[1,2,3], YU GU[1,3], YANG LIU[1], XIANJING MENG[1], AND JING LI[1]

[1]Inner Mongolia Key Laboratory of Pattern Recognition and Intelligent Image Processing, School of Information Engineering, Inner Mongolia University of Science and Technology, Baotou 014010, China
[2]School of Information Engineering, Inner Mongolia University of Technology, Hohhot 010051, China
[3]School of Computer Engineering and Science, Shanghai University, Shanghai 200444, China

Corresponding authors: Xiaoqi Lu (lxiaoqi@imut.edu.cn) and Yu Gu (guyu2010023@imust.edu.cn)

This work was supported in part by the National Natural Science Foundation of China under Grant61841204, Grant 61771266, and Grant 61179019, in part by the Inner Mongolia Natural Science Foundation under Grant 2015MS0604, and in part by the Inner Mongolia College Science and Technology Research Project under Grant NJZY145.

ABSTRACT Iris segmentation plays an important role in the iris recognition system, and the accurate segmentation of iris can lay a good foundation for the follow-up work of iris recognition and can improve greatly the efficiency of iris recognition. We proposed four new feasible network schemes, and the best network model fully dilated convolution combining U-Net (FD-UNet) is obtained by training and testing on the same datasets. The FD-UNet uses dilated convolution instead of original convolution to extract more global features so that the details of images can be processed better. The proposed method is tested in the near-infrared illumination iris datasets (CASIA-iris-interval-v4.0 and ND-IRIS-0405) and the visible light illumination iris dataset (UBIRIS.v2). The f1 scores of our model on the CASIA-iris-interval-v4.0, ND-IRIS-0405, and UBIRIS.v2 datasets reached 97.36%, 96.74%, and 94.81%, respectively. The experimental results show that our network model improves the accuracy and reduces the error rate, which performs well on both near-infrared illumination and visible light illumination iris datasets with good robustness.

INDEX TERMS Iris recognition, biometrics, image segmentation, convolutional neural network, deep learning.

I. INTRODUCTION

With the development of information technology, identity recognition is becoming increasingly difficult and important. Traditional identification methods include password, Identity Card and so on, but they no longer meet the needs of modern society with defects of easy to lose, easy to be forged, easy to be cracked, etc. Biometric identification has the advantages of being stable, convenient and not easy to be forged, and it is easier to integrate computer with security, monitoring and management systems to achieve automatic management, which has become a hot spot in recent years. Traditional biometrics includes fingerprint, face, voice, handwriting and so on. However, these traditional biometrics technologies have more or less defects that will bring great hidden losses or even irreversible danger to the protected. The iris-based biometric technology, relying on the uniqueness, stability and reliability of iris texture, can bring people a more convenient, safe and efficient experience.

Most iris recognition systems include five basic steps: iris image acquisition, preprocessing, iris boundary segmentation, iris feature extraction and iris matching verification or identification. In the process of iris recognition, it is very important to segment the iris accurately. By choosing the right iris region, we can extract the valuable information from the iris image and further improve the accuracy of the iris recognition system. This paper presents an automatic iris segmentation method based on U-Net, which uses popular datasets and ground truth images for training and testing. It is verified that our network model can achieve high precision in iris segmentation in four datasets. Our main innovations and contributions are as follows:

1) A novel network model combining U-Net and dilated convolution is proposed for iris image segmentation. Combined with the advantages of dilated convolution, more image feature information can be extracted and the segmentation accuracy can be improved

The associate editor coordinating the review of this manuscript and approving it for publication was Kien Nguyen.

2) Four new feasible network schemes are proposed, and the best network model FD-UNet is obtained by training and testing on the same datasets
3) Results on the near-infrared illumination iris datasets and the visible light illumination iris datasets further verify that FD-UNet has better network performance.

The rest of this paper is organized as follows: section 2 introduces the related work of iris segmentation, including traditional algorithms and deep-learning-based algorithms. Section 3 introduces four proposed network models. Section 4 describes the implementation of our experiment, including datasets and experimental results. Section 5 compares our approach with those of others to verify the effectiveness of our approach.

II. RELATED WORK

A. CONVENTIONAL METHOD

Iris segmentation is to accurately locate the iris region in the iris image. In the early time, iris segmentation was based on the concept that the pupil and the iris edge in an iris image are approximately circular. Bowyer *et al.* [1] reviewed the literatures on iris biometrics. Daugman and John [2] used the calculus operator as the circular edge detector and segmented the iris by fitting the circular boundary of pupil and iris. He *et al.* [3] built Adaboost-cascade iris detectors and an elastic model named 'pulling and pushing method' to segment the iris. The classic iris segmentation algorithms also involved detecting iris boundaries using Hough Transform [4]–[6]. But all of these methods require high-quality iris images, and need a clear and regular shape of iris boundaries. However, the acquisition of iris images is not always in an ideal environment. For the non-ideal iris images, there are some noises such as blur, glasses occlusion, and so on. It performs well in non-ideal environments using machine learning techniques to segment the iris. Gangwar *et al.* [7] and Haindl and Krupička [8] used the techniques of adaptive filtering and adaptive threshold to propose a segmentation framework for non-ideal iris images, and achieved good results.

B. CONVOLUTIONAL NEURAL NETWORK (CNN) FOR IRIS SEGMENTATION

In recent years, with the appearance of deep learning theory, more and more researchers apply it to iris image segmentation [9]–[13]. CNN is a typical network structure in deep learning. CNN can be used to segment the iris image, which reduces the procedures of iris feature extraction and feature selection to further improve the segmentation accuracy.

Hierarchical Convolutional Neural Network (HCNN) and Multi-scale Fully Convolution Network (MFCN) was proposed by Liu *et al.* [14] to deal with noisy iris images acquired in long distance and in motion. Jalilian and Uhl [15] proposed three types of Fully Convolution Encoder-Decoder Networks (FCEDN) for iris segmentation. Yang *et al.* [16] proposed a network model combining FCN with dilated convolution to segment iris, and trained and tested it on CASIA-iris-interval-v4.0, UBIRIS.v2 and IITD Delhi datasets with 98.6%, 98.4% and 95.7% accuracy, respectively. Bazrafkan *et al.* [17] proposed an end-to-end convolutional neural network for low-quality iris image segmentation with good results. Lozej *et al.* [18] implemented end-to-end iris segmentation using U-Net model. Hofbauer *et al.* [19] marked iris images for iris segmentation, and their public data will be used in our work.

III. MODELS AND METHODS

A. DILATED CONVOLUTION

Yu and Koltun [20] have proposed a new method called dilated convolution, which can be used in the field of image segmentation. It can obtain more receptive field information without increasing the complexity of the algorithm and losing the information. The global information of the image can be utilized. The basic principle is as shown as Figure 1. For the conventional convolution kernel, a value of 0 is inserted between each pixel to increase the receptive field when the original convolution kernel is set to 3×3. The dilated convolution kernel is 3×3 when the dilation rate $r = 1$, and the dilated convolution kernel is 5×5 when $r = 2$.

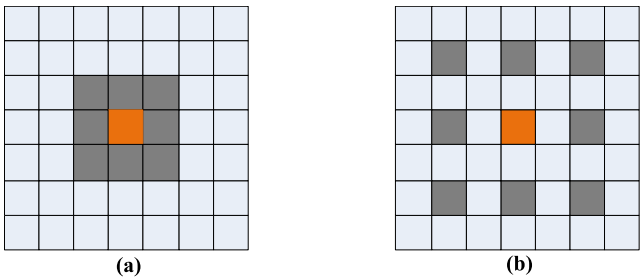

FIGURE 1. Dilated Convolution diagram. (a)When r = 1, convolution kernel is 3 × 3 (b) When r = 2, convolution kernel is 5 × 5.

B. NETWORK DESIGN

The U-Net network model forms a u-shaped structure with a contraction path and an expansion path [21]. The contraction path is mainly responsible for pooling and extracting feature information. Each pooling goes through two 3×3 unpadded convolution operations and a 2×2 pool operation, which makes the size of the image become 1 / 2 of the original size and the number of feature channels becomes twice the original. The expansion path is mainly responsible for up-sampling. The size of the image is doubled and the number of feature channels is reduced to 1 / 2 by Rectified Linear Unit (ReLU) as the activation function after two 3×3 convolution operations. In the process of up-sampling, the output features of each time are combined with the features of the corresponding contraction path to complete the lost information. Finally, a convolution operation with a convolution kernel of 1×1 is added to map the previously acquired features to the category to which they belong.

1) PART DILATED CONVOLUTION COMBINING U-NET (PD-UNET)

The pool operation in the U-Net contraction path reduces the size of the image, and the corresponding up-sampling

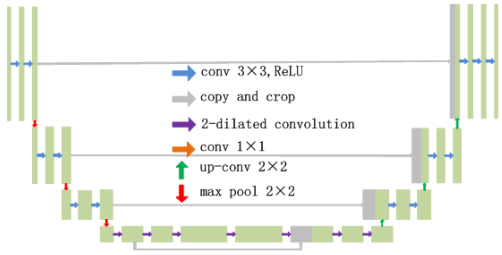

(a)Part Dilated Convolution Combine UNet 1(PD-UNet1). Based on U-Net, we reserve the convolution, pooling and up-sampling parts corresponding to first three copy and crop operations in the model. Then we use dilation convolutions with a dilation rate of 2 to replace the rest convolution, pooling and up-sampling operations.

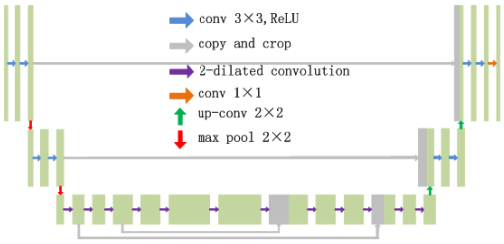

(b)Part Dilated Convolution Combine UNet 2(PD-UNet2). Based on U-Net, we reserve the convolution, pooling and up-sampling parts corresponding to first two copy-and-crop operations in the model. Then we use dilation convolutions with a dilation rate of 2 to replace the rest convolution, pooling and up-sampling operations.

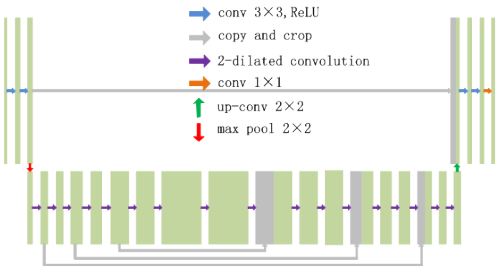

(c)Part Dilated Convolution Combine UNet 3(PD-UNet3). Based on U-Net, we reserve the convolution, pooling and up-sampling parts corresponding to first two copy-and-crop operations in the model. Then we use dilation convolutions with a dilation rate of 2 to replace the rest convolution, pooling and up-sampling operations.

FIGURE 2. Network model of part dilated convolution combining U-Net.

operation will restore the image to its original size, but some details will be lost. To solve this problem, Part Dilated Convolution combining U-Net (PD-UNet) is proposed, and its network model is shown in Figure 2. We use dilation convolutions with a dilation rate of 2 to replace part of convolution, pooling and up-sampling operations.

2) FULLY DILATED CONVOLUTION COMBINING U-NET (FD-UNET)

In U-Net network, there exists the problem of missing boundary with every 3 × 3 unpadded convolution operation. The dilated convolution can increase the receptive field of the convolution kernel while keeping the number of parameters unchanged to get more details about the image. Thus, Fully Dilated Convolution combining U-Net (FD-UNet) is presented, and its network model is shown in Figure 3. The network model retains all pooling and up-sampling operations in U-Net, and replaces all the 3 × 3 unpadded convolutions in U-Net with 2-dilated convolutions except for the 1x1 convolution in the last layer.

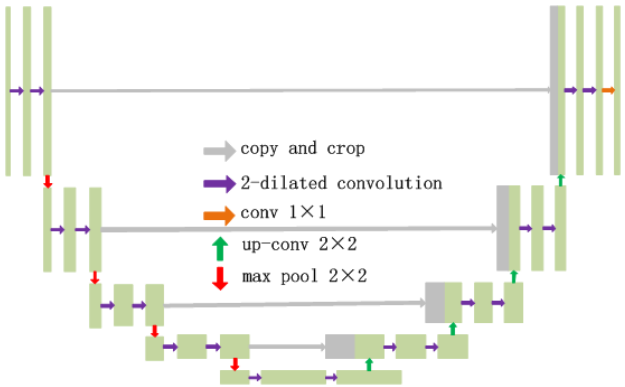

FIGURE 3. Network model of fully dilated convolution combining U-Net. Based on U-Net, we reserve all pooling and up-sampling operations, and replace all the 3 × 3 unpadded convolutions in U-Net with 2-dilated convolutions except for 1 x 1 convolution in the last layer.

IV. EXPERIMENT

A. EXPERIMENT DATA

Our work uses CASIA-4i, ND-IRIS-0405 and UBIIRIS.v2 datasets. The iris images of CASIA-4i, ND-IRIS-0405 dataset was obtained under near-infrared illumination. The iris images of the UBIRIS.v2 dataset were taken under visible light illumination. The iris ground truth images in these datasets were provided by Hofbauer *et al.* [19].

CASIA-iris-interval-v4.0[22]: CASIA-iris-interval-v4.0 (CASIA-4i) dataset belongs to a subset of the CASIA database. The dataset was collected in indoor environment using a close-range infrared iris camera with a circular NIR LED array. Therefore the image has very clear iris texture details. The dataset has an iris image pixel of 320 × 280.

ND-IRIS-0405[23]: The iris images of this dataset were collected in a controlled environment with little change, and we used a small portion of the original dataset. The iris image pixels in the database are 640 × 480.

UBIRIS.v2 Database[24]: This dataset is an iris database obtained in an unconstrained environment using visible light illumination. The library's iris images, captured by the

Nikon E5700 camera, contain front and offset iris images with occlusion at various distances. Iris image pixels are 400 × 300.

The iris ground truth images from the four datasets provided by Hofbauer *et al.* [19] are used. The ground truth images of iris segmentation are obtained based on the boundary points of lower and upper eyelids and the inner and outer circumferences of the irises. A ground truth images database for iris segmentation and a method for evaluating iris segmentation algorithms using ground truth datasets are provided by Hofbauer et al. as well. Our iris segmentation methods are evaluated by these datasets.

B. EVALUATION CRITERIA

The above networks in section ćó were trained and tested on CASIA-4i, ND-IRIS-0405 and UBIRIS.v2 datasets, and network performance was analyzed. The aim of the segmentation algorithm is to retrieve the iris region from the image. We divide the iris segmentation results into four types, as shown in Figure 4. Among them, True Positive (TP) indicates the number of iris image pixels which are correctly segmented, and False Positive (FP) indicates the number of iris image pixels incorrectly segmented. False Negative (FN) indicates the number of unrecognized iris image pixels in the segmentation result, and True Negative (TN) indicates the number of unrecognized non-iris pixels in the segmentation result.

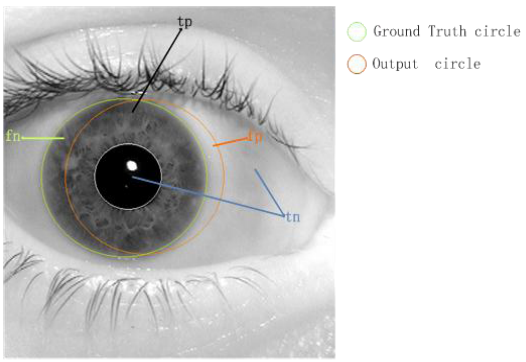

FIGURE 4. Iris Segmentation Results Sketch Map.

To evaluate the performance of the proposed networks, the nice1 score and nice2 score of the NICE 1 contest [25] were used. In addition, we used f1 score to evaluate the accuracy of our segmentation results.

The nice1 score is widely used to evaluate the error rate of iris segmentation. The segmentation error fraction nice1 is the ratio of the inconsistent pixels (by a logical XOR operation) of the resulting image to all the pixels in the image. It is defined as follows:

$$nice1 = \frac{1}{N \times m \times n} \sum_{k=1}^{N} \sum_{i,j \in (m,n)} G(i,j) \oplus O(i,j) \qquad (1)$$

where N is the number of images and (m, n) is the spatial resolution of the image. G (i, j) and O (i, j) represent the pixels of the ground truth image and the output image, respectively.

The nice2 is also an error score, which is obtained by averaging the False Positive Rate (FPR) and False Negative Rate (FNR). FNR and FPR are defined as follows:

$$FNR = \frac{FN}{FN + TP} \qquad (2)$$

$$FPR = \frac{FP}{FP + TN} \qquad (3)$$

The formula of nice2 is as followsčž

$$nice2 = \frac{1}{2}(FPR + FNR) \qquad (4)$$

The f1 value is the harmonic average of the precision and recall which can represent the accuracy of model segmentation, and its formula is defined as follows:

$$f1 = \frac{2TP}{2TP + FP + FN} \qquad (5)$$

C. EXPERIMENT

1) EXPERIMENT I

The aim of Experiment I is to get the network with best performance among the four feasible schemes. The segmentation results of our proposed network models on CASIA-4i dataset are shown in Figure 5 and Figure 6. First of all, the error scores of nice1 and nice2 are less than 1% and 2.5% respectively, and the accuracy of f1 is more than 96%, which shows that the proposed method has high accuracy and low error rate. Secondly, with the increase of convolution instead of pooling, the accuracy of U-Net, PD-UNet1, PD-UNet2 and PD-UNet3 are 97.23%, 96.82%, 96.70% and 96.28% respectively, the nice1 of U-Net, PD-UNet1, PD-UNet2 and PD-UNet3 are 0.61%, 0.70%, 0.72 and 0.83% respectively, the nice2 of U-Net, PD-UNet1, PD-UNet2 and PD-UNet3 are 1.27%, 1.45%, 1.61 and 2.23% respectively. Finally, among the four feasible schemes, the performance of FD-UNet is the best in iris segmentation. The nice1 and nice2 scores of

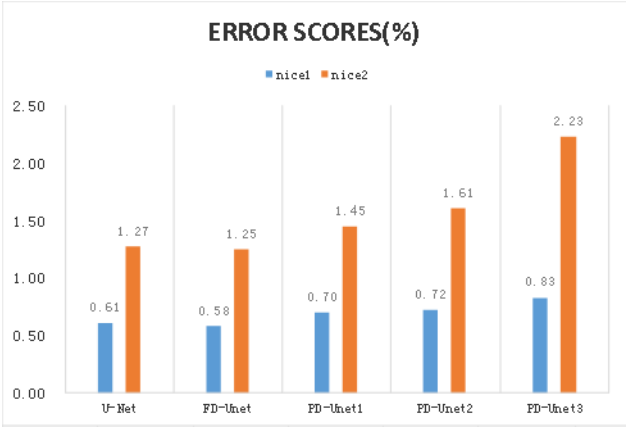

FIGURE 5. Error scores for five networks.

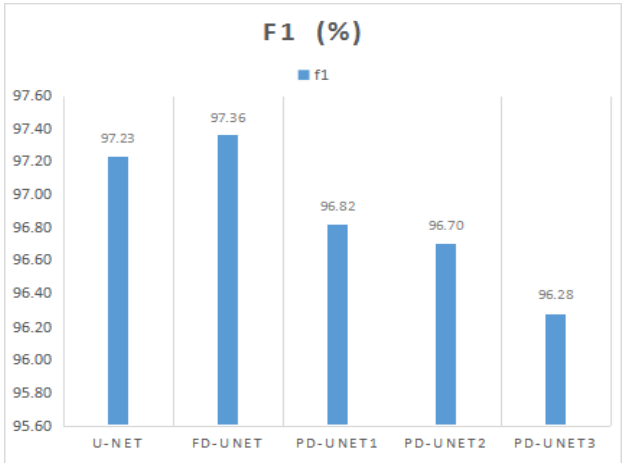

FIGURE 6. f1 values for five networks.

FD-UNet are 0.58%, 1.25% respectively, which are smaller than those of U-Net, and its f1 score is 97.36%, which is higher than that of U-Net.

The results show that FD-UNet has higher accuracy than that of PD-UNet in iris segmentation and can get more accurate segmentation results.

2) EXPERIMENT II

In Experiment II, FD-UNet and U-Net are trained and tested on three different datasets to prove that FD-UNet's network model has better performance in iris segmentation. Figure 7 is the result of FD-UNet's iris segmentation on the three datasets. The first column shows the input images, the second column shows the ground truth images and the third column shows the output images. The images in the first row are from the CASIA-4i dataset, the images in the second row are from the ND-IRIS-0405 dataset, and the images in the third and fourth rows are from the UBIRIS.v2 dataset. In the second row of iris image, the spot between iris and eyelid is not marked in the tagged image, but our network can be trained to segment it into non-iris. The iris image in the third row is a noisy iris image occluded by glasses, and our network can still segment the iris well after training.

Table 1 shows the results of our method on three datasets. The nice1 and nice2 error scores of FD-UNet segmentation results are lower than those of U-Net, and the f1 scores of FD-UNet segmentation are higher than those of U-Net, which shows that the performance of the proposed network is better than U-Net. At the same time, our method performs well in all three datasets with f1 values greater than 94%, indicating that our method is suitable for both near-infrared illumination and visible light illumination iris images.

During the training, it is important to achieve accuracy close to 1 and a loss close to 0. Figure 8 (a), (b) show the training accuracy and training loss curves of U-Net and FD-UNet by experimenting on the CASIA-4i dataset. The x-axis for each curve shows the number of epochs and the y-axis shows the training accuracy and loss. The experimental

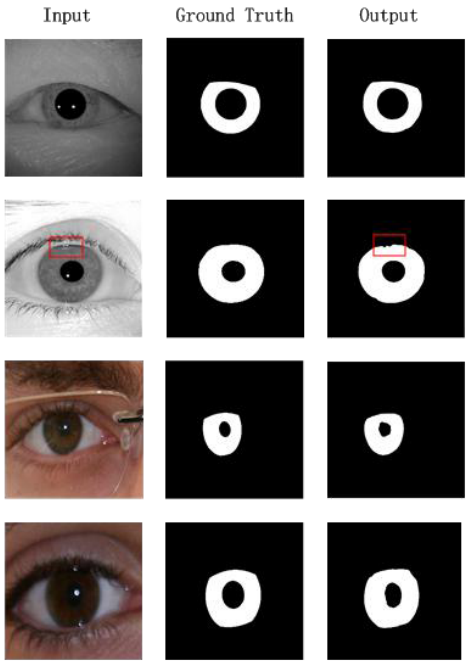

FIGURE 7. Segmentation results by FD-UNet.

TABLE 1. Results on the three datasets.

Dataset	Method	nice1(%)	nice2(%)	f1(%)
CASIA-4i	U-Net	0.61	1.27	97.23
	FD-UNet	0.58	1.25	97.36
ND-IRIS-0405	U-Net	0.65	4.81	92.88
	FD-UNet	0.18	1.73	96.74
UBIRIS.v2	U-Net	0.50	3.00	93.48
	FD-UNnet	0.40	2.58	94.81

results show that the FD-UNet network can reach a higher accuracy and a much lower loss value, and converges faster during the training process. And the loss value of FD-UNet drops significantly faster and reaches a lower value. Thus, FD-UNet has better network performance.

V. DISCUSSION

The proposed method is compared with the traditional algorithms [26]–[29] and the CNN iris segmentation methods [15]–[17], [30] on the premise of using the same dataset and the same tagged image data. Tables 2 and 3 show the segmentation results of these methods on the near-infrared illumination iris dataset; Table 4 shows the segmentation results of these methods on the visible light illumination iris dataset.

Table 2 shows the segmentation results of these methods on the CASIA-4i dataset. In the traditional method, Wahet's

TABLE 2. Results on CASIA-4I dataset.

Methods		nice1(%)	nice2(%)	f1(%)
Traditional algorithm for iris segmentation	Wahet[26]	6.08	8.42	89.49
	Caht[27]	11.61	14.70	76.51
	Ifpp[28]	15.32	23.72	62.78
	Osiris[29]	5.56	6.73	88.62
CNN for iris segmentation	FCEDNs-origianal[15]	5.61	5.88	88.26
	FCEDNs-basic[15]	4.48	4.38	90.72
	FCEDNs-bayesian-basic[15]	3.91	4.07	91.92
	Yang[16]	0.79	0.88	98.6
	Shabab[17]	-	-	97.50
	Ahmad[30]	-	-	95.80
	U-Net	0.61	1.27	97.23
Proposed	**FD-UNet**	**0.58**	**1.25**	**97.36**

TABLE 3. Results on ND-IRIS-0405 dataset.

Methods	nice1(%)	nice2(%)	f1(%)
Ahmad[30]	-	-	95.2
U-Net	0.22	1.73	95.93
FD-UNet	**0.18**	**1.56**	**96.74**

TABLE 4. Results on UBIRIS.v2 dataset.

Methods		nice1(%)	nice2(%)	f1(%)
Traditional algorithm for iris segmentation	Wahet[26]	27.43	44.98	19.77
	Caht[27]	12.26	48.09	10.48
	Ifpp[28]	23.79	39.70	28.99
	Osiris[29]	18.27	40.95	23.28
CNN for iris segmentation	FCEDNs-origianal[15]	3.42	12.49	79.61
	FCEDNs-basic[15]	4.23	15.17	77.0
	FCEDNs-bayesian-basic[15]	3.06	11.16	84.07
	Yang[16]	0.64	1.73	95.7
	Shabab[17]	-	-	93.90
	Ahmad[30]	-	-	94.60
	U-Net	0.50	3.00	93.48
Proposed	**FD-UNet**	**0.40**	**2.58**	**94.81**

method performs the best. However, compared with it, the nice1, nice2 and f1 of FD-UNet is improved by 5.50%, 7.17% and 7.19% respectively. In the CNN iris segmentation method, FD-UNet has better performance than the three types of FCEDN proposed by Jalilian and Uhl [15]. Compared with FCEDNs-bayesian-basic, the nice1, nice2, and f1 score of our method are improved by 3.33%, 2.82%, and by 5.44%, respectively. Also, our method is 1.56% better than Ahmad and Fuller [30] in f1 score, and our f1 score is similar to that of Shabab [17]. Compared with Yang et al., our method scores 0.37% lower in nice2, and the f1 score is also 1.24% lower, but the nice1 score is increased by 0.21%.

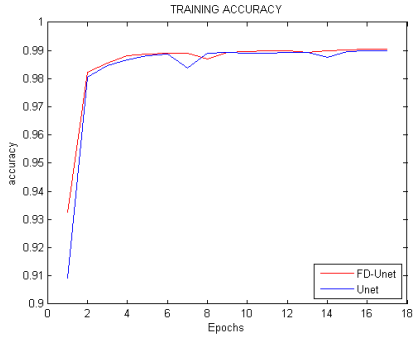

(a)

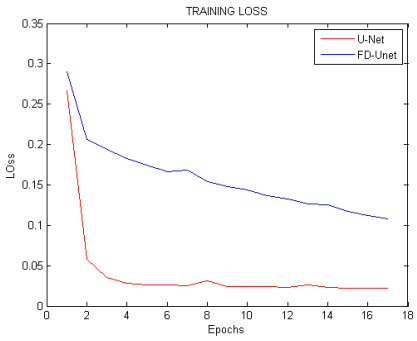

(b)

FIGURE 8. Training accuracy and loss curves of U-Net and FD-UNet. (a) Training accuracy of U-Net and FD-UNet. (b) Training loss of U-Net and FD-UNet.

Table 3 shows the segmentation results of these methods on the ND-IRIS-0405 dataset. On this dataset, the f1 score of our method is 1.54% better than that of Ahmad et al.'s method.

Table 4 shows the segmentation results of these methods on the UBIRIS.v2 dataset. Compared with Wahet's method, our nice1 nice2 and f1 score is improved by 27.03%, 42.40% and 75.04% respectively. Meantime, compared with FCEDNs-bayesian-basic, the score of our model for nice1, nice2 and f1 is improved by 2.66%, 8.58% and 10.74% respectively. Our f1 score is 0.91% and 0.21% higher than the score of Shabab's method and Ahmad's method, respectively. Also, the nice2 and f1 score of ours is improved by 0.85% and 0.89% compared with Yang's, but the nice1 score is 0.24% higher.

The results show that our method can effectively improve the iris segmentation performance on the near-infrared illumination iris dataset. Furthermore, on the visible light illumination iris dataset with more noise, the result of segmentation is also improved. The results show that our method has better robustness.

VI. CONCLUSION

Iris segmentation plays a vital role in the whole iris recognition system. In order to improve the accuracy of iris segmentation, a more accurate iris segmentation algorithm is proposed, which can realize the end-to-end iris segmentation. Combining the dilated convolution with U-Net network, the dilated convolution operation can extract more image information, obtain more details, and improve both the network performance and the accuracy of iris segmentation. Our network model is trained and tested on three different iris datasets with different types of near-infrared illumination and visible light illumination, and the network is evaluated by three popular segmentation scores. At the same time, our method is compared with the traditional methods and CNN iris segmentation methods. The results show that our network model improves the accuracy and reduces the error rate.

The plans of future research work are as follows: first, adjust network parameters to obtain better network performance and to improve segmentation accuracy. Second, we can obtain a more promising network model by combining better performing network models. Through these improvements, network performance will be further improved.

ACKNOWLEDGEMENT

The authors would like to thank the Chinese Academy of Sciences, the University of Notre Dame du Lac, and the University of Beira Interior for providing the iris databases. They would also like to thank Hofbauer *et al.* for providing the iris ground truth images.

REFERENCES

[1] K. W. Bowyer, K. P. Hollingsworth, and P. J. Flynn, "A survey of iris biometrics research: 2008–2010," in *Handbook of Iris Recognition*. London, U.K.: Springer, 2013, pp. 15–54.
[2] J. G. Daugman, "High confidence visual recognition of persons by a test of statistical independence," *IEEE Trans. Pattern Anal. Mach. Intell.*, vol. 15, no. 11, pp. 1148–1161, Nov. 1993.
[3] Z. He, T. Tan, Z. Sun, and X. Qiu, "Toward accurate and fast iris segmentation for iris biometrics," *IEEE Trans. Pattern Anal. Mach. Intell.*, vol. 31, no. 9, pp. 1670–1684, Sep. 2009.
[4] L. Ma, Y. Wang, and T. Tan, "Iris recognition using circular symmetric filters," in *Proc. Object Recognit. Supported Interact. Service Robots*, vol. 2, Aug. 2002, pp. 414–417.
[5] W. K. Kong and D. Zhang, "Accurate iris segmentation based on novel reflection and eyelash detection model," in *Proc. Int. Symp. Intell. Multimedia, Video Speech Process.*, May 2001, pp. 263–266.
[6] R. P. Wildes, J. C. Asmuth, K. J. Hanna, S. C. Hsu, R. J. Kolczynski, J. R. Matey, S. E. McBride, "Automated, non-invasive iris recognition system and method," U.S. Patent, 55 725 96A, May 11, 1996.
[7] A. Gangwar, A. Joshi, A. Singh, F. Alonso-Fernandez, and J. Bigun, "IrisSeg: A fast and robust iris segmentation framework for non-ideal iris images," in *Proc. Int. Conf. Biometrics (ICB)*, Jun. 2016, pp. 1–8.
[8] M. Haindl and M. Krupička, "Unsupervised detection of non-iris occlusions," *Pattern Recognit.*, vol. 57, pp. 60–65, May 2015.
[9] F. Zhao, Y. Chen, F. Chen, X. He, X. Cao, Y. Hou, H. Yi, X. He, and J. Liang, "Semi-supervised cerebrovascular segmentation by hierarchical convolutional neural network," *IEEE Access*, vol. 6, pp. 67841–67852, 2018.
[10] Y. Gu, X. Lu, L. Yang, B. Zhang, D. Yu, Y. Zhao, L. Gao, L. Wu, and T. Zhou, "Automatic lung nodule detection using a 3D deep convolutional neural network combined with a multi-scale prediction strategy in chest CTs," *Comput. Biol. Med.*, vol. 103, pp. 220–231, Dec. 2018.
[11] C. Feng, Y. Sun, and X. Li, "Iris R-CNN: Accurate iris segmentation in non-cooperative environment," Mar. 2019, *arXiv:1903.10140*. [Online]. Available: https://arxiv.org/abs/1903.10140
[12] Z. Zeng, W. Xie, Y. Zhang, and Y. Lu, "RIC-Unet: An improved neural network based on Unet for nuclei segmentation in histology images," *IEEE Access*, vol. 7, pp. 21420–21428, 2019.

[13] Y. Gu, X. Lu, B. Zhang, Y. Zhao, D. Yu, L. Gao, G. Cui, L. Wu, and T. Zhou, "Automatic lung nodule detection using multi-scale dot nodule-enhancement filter and weighted support vector machines in chest computed tomography," *PLoS ONE*, vol. 14, no. 1, Jan. 2019, Art. no. e0210551.

[14] N. Liu, H. Li, M. Zhang, J. Liu, Z. Sun, and T. Tan, "Accurate iris segmentation in non-cooperative environments using fully convolutional networks," in *Proc. Int. Conf. Biometrics (ICB)*, Jun. 2016, pp. 1–8.

[15] E. Jalilian and A. Uhl, "Iris segmentation using fully convolutional encoder–decoder networks," in *Deep Learning for Biometrics*. Cham, Switzerland: Springer, 2017, pp. 133–155.

[16] Y. Yang, P. Shen, and C. Chen, "A robust iris segmentation using fully convolutional network with dilated convolutions," in *Proc. IEEE Int. Symp. Multimedia (ISM)*, Dec. 2018, pp. 9–16.

[17] S. Bazrafkan, S. Thavalengal, and P. Corcoran, "An end to end deep neural network for iris segmentation in unconstrained scenarios," *Neural Netw.*, vol. 106, pp. 79–95, Oct. 2018.

[18] J. Lozej, B. Meden, V. Struc, and P. Peer, "End-to-end iris segmentation using U-net," in *Proc. IEEE Int. Work Conf. Bioinspired Intell. (IWOBI)*, Jul. 2018, pp. 1–6.

[19] H. Hofbauer, F. Alonso-Fernandez, P. Wild, J. Bigun, and A. Uhl, "A ground truth for iris segmentation," in *Proc. 22nd Int. Conf. Pattern Recognit.*, Aug. 2014, pp. 527–532.

[20] F. Yu and V. Koltun, "Multi-scale context aggregation by dilated convolutions," Nov. 2015, *arXiv:1511.07122*. [Online]. Available: https://arxiv.org/abs/1511.07122

[21] O. Ronneberger, P. Fischer, and T. Brox, "U-net: Convolutional networks for biomedical image segmentation," in *Proc. Int. Conf. Med. Image Comput. Comput.-Assist. Intervent.* Cham, Switzerland: Springer, Nov. 2015, pp. 234–241.

[22] Biometrics Ideal Test. *CASIA.v4 Database*. Accessed: 2002. [Online]. Available: http://biometrics.idealtest.org

[23] P. J. Phillipm, W. T. Scruggs, A. J. O'Toole, P. J. Flynn, K. W. Bowyer, C. L. Schott, and M. Sharpe, "FRVT 2006 and ICE 2006 large-scale experimental results," *IEEE Trans. Pattern Anal. Mach. Intell.*, vol. 32, no. 5, pp. 831–846, May 2010.

[24] H. Proenca, S. Filipe, R. Santos, J. Oliveira, and L. A. Alexandre, "The UBIRIS.v2: A database of visible wavelength iris images captured on-the-move and at-a-distance," *IEEE Trans. Pattern Anal. Mach. Intell.*, vol. 32, no. 8, pp. 1529–1535, Aug. 2010.

[25] (2009). *NICE.I-Noisy Iris Challenge Evaluation, Part I*. [Online]. Available: http://nice1.di.ubi.pt/index.html

[26] A. Uhl and P. Wild, "Weighted adaptive Hough and ellipsopolar transforms for real-time iris segmentation," in *Proc. 5th IAPR Int. Conf. Biometrics (ICB)*, Mar./Apr. 2012, pp. 283–290.

[27] C. Rathgeb, A. Uhl, and P. Wild, *Iris Biometrics: From Segmentation to Template Security*, vol. 59. Springer, 2012.

[28] P. Wild, H. Hofbauer, J. Ferryman, and A. Uhl, "Segmentation-level fusion for iris recognition," in *Proc. Int. Conf. Biometrics Special Interest Group (BIOSIG)*, Sep. 2015, pp. 1–6.

[29] D. Petrovska and A. Mayoue, "Description and documentation of the biosecure software library," Project no. IST-2002-507634-BioSecure, Deliverable, 2007.

[30] S. Ahmad and B. Fuller, "Unconstrained iris segmentation using convolutional neural networks," Dec. 2018, *arXiv:1812.08245*. [Online]. Available: https://arxiv.org/abs/1812.08245

WEI ZHANG is currently pursuing the M.S. degree with the Inner Mongolia Key Laboratory of Pattern Recognition and Intelligent Image Processing, School of Information Engineering, Inner Mongolia University of Science and Technology, Baotou, China. Her research interests include pattern recognizing and medical image processing.

XIAOQI LU received the M.S. degree in medical information processing from Xi'an Jiaotong University, Xi'an, China, in 1989, and the Ph.D. degree in control theory and control engineering from the Beijing University of Science, Beijing, China, in 2003, respectively. He is currently a Professor with the Inner Mongolia University of Technology, Hohhot, China. His research interests include intelligent image processing, pattern recognizing, and neural networks.

YU GU received the master's degree in control science and engineering from the Inner Mongolia University of Science and Technology, China. He is currently pursuing the Ph.D. degree in computer science and engineering with Shanghai University, China. He is currently an Associate Professor with the School of Information Engineering, Inner Mongolia University of Science and Technology. His main research interests include machine learning and medical image processing.

YANG LIU is currently pursuing the M.S. degree with the School of Information Engineering, Inner Mongolia University of Science and Technology, Baotou, China. His research interests include pattern recognizing and medical image processing.

XIANJING MENG is currently pursuing the M.S. degree with the School of Information Engineering, Inner Mongolia University of Science and Technology, Baotou, China. Her research interests include pattern recognizing and medical image processing.

JING LI received the M.S. degree from the Inner Mongolia University of Science and Technology, Baotou, China, in 2002. Her research interest includes computer technology.